Final piece to the Fusarium pigmentation puzzle – Unraveling of the phenalenone biosynthetic pathway responsible for perithecial pigmentation in the Fusarium solani species complex

Nielsen, Mikkel Rank; Sørensen, Trine; Pedersen, Tobias Bruun; Westphal, Klaus Ringsborg; Fernandez de Quincoces, Lorena Diaz ; Sondergaard, Teis Esben; Wimmer, Reinhard; Brown, Daren W.; Sørensen, Jens Laurids

Published in:
Fungal Genetics and Biology

DOI (link to publication from Publisher):
10.1016/j.fgb.2024.103912

Publication date:
2024

Document Version
Publisher's PDF, also known as Version of record

Fungal Genetics and Biology 174 (2024) 103912

Contents lists available at ScienceDirect

Fungal Genetics and Biology

journal homepage: www.elsevier.com/locate/yfgbi

Regular Articles

Final piece to the Fusarium pigmentation puzzle – Unraveling of the phenalenone biosynthetic pathway responsible for perithecial pigmentation in the Fusarium solani species complex

Mikkel Rank Nielsen [a], Trine Sørensen [b], Tobias Bruun Pedersen [a], Klaus Ringsborg Westphal [b], Lorena Díaz Fernández De Quincoces [a], Teis Esben Sondergaard [b], Reinhard Wimmer [b], Daren W. Brown [c], Jens Laurids Sørensen [a,*]

[a] Department of Chemistry and Bioscience, Aalborg University, Niels Bohrs Vej 8A, 6700 Esbjerg, Denmark
[b] Department of Chemistry and Bioscience, Aalborg University, Fredrik Bajers Vej 7H, 9220 Aalborg, Denmark
[c] National Center for Agricultural Utilization Research, U.S. Department of Agriculture, 1815 N University St. Peoria IL 61604, United States of America

ARTICLE INFO

Keywords:
Heterologous expression
Pigments
Fusarium vanettenii
Corymbiferan lactone
Perithecia
Polyketides

ABSTRACT

The *Fusarium solani* species complex (FSSC) is comprised of important pathogens of plants and humans. A distinctive feature of FSSC species is perithecial pigmentation. While the dark perithecial pigments of other *Fusarium* species are derived from fusarubins synthesized by polyketide synthase 3 (PKS3), the perithecial pigments of FSSC are derived from an unknown metabolite synthesized by PKS35. Here, we confirm in FSSC species *Fusarium vanettenii* that PKS35 (*fsnI*) is required for perithecial pigment synthesis by deletion analysis and that *fsnI* is closely related to *phnA* from *Penicillium herquei*, as well as *duxI from Talaromyces stipentatus*, which produce prephenalenone as an early intermediate in herqueinone and duclauxin synthesis respectively. The production of prephenalenone by expression of *fsnI* in *Saccharomyces cerevisiae* indicates that it is also an early intermediate in perithecial pigment synthesis. We next identified a conserved cluster of 10 genes flanking *fsnI* in *F. vanettenii* that when expressed in *F. graminearum* led to the production of a novel corymbiferan lactone F as a likely end product of the phenalenone biosynthetic pathway in FSSC.

1. Introduction

The *Fusarium solani* species complex (FSSC) is one of the most widespread fungal groups with members causing disease in both plants and humans (Coleman, 2016; Zhang et al., 2006). More than 50 species within the FSSC have been described (O'Donnell, 2000; O'Donnell et al., 2008; Zhang et al., 2006) and new species are identified each year (Šišić et al., 2018a). FSSC members are important plant pathogens of more than 100 agricultural crops where they can cause vascular wilt or root rot (Kolattukudy and Gamble, 1995). The association of some *F. solani* strains to one or a few hosts has led to their assignment to formae speciales (Bueno et al., 2014; Chung et al., 2011; Suga et al., 2002), although this view has been challenged (Šišić et al., 2018b). Variation within the species complex is also reflected in their varied reproductive abilities as strains may be heterothallic or homothallic or produce spores asexually (O'Donnell, 2000). In contrast to the colorless asexual spores, sexual spores and perithecia often appear reddish or orangish due to an unknown polyketide pigment (Nalim et al., 2011).

Fusarium pigmentation is due primarily to four polyketide synthase (PKS) gene clusters. Mycelial pigmentation is mediated by aurofusarin or bikaverin, which are synthesized by the PKS12 (Frandsen et al., 2006; Kim et al., 2005; Malz et al., 2005) and PKS16 gene clusters, respectively (Linnemannstöns et al., 2002; Wiemann et al., 2009). Most perithecial pigmentation is mediated by fusarubins and bostrycoidins which are synthesized by the *PKS3* gene cluster (Awakawa et al., 2012; Frandsen et al., 2016; Studt et al., 2012). However, in FSSC species fusarubins and bostrycoidins mediate mycelial pigmentation (Arnstein and Cook, 1947; Hardegger et al., 1964; Parisot et al., 1990; Ruelius and Gauhe, 1950) while perithecial pigmentation is mediated by an unknown chemical synthesized by the *PKS35* gene cluster (Brown and Proctor, 2016; Graziani et al., 2004). The presence of PKS35 homologs in members of *Fusarium* species complexes basal to FSSC suggest the production of this

* Corresponding author at: Aalborg University Esbjerg, Department of Chemistry and Bioscience, Niels Bohrs Vej 8, 6700 Esbjerg, Denmark.
E-mail address: jls@bio.aau.dk (J.L. Sørensen).

https://doi.org/10.1016/j.fgb.2024.103912
Received 18 April 2024; Received in revised form 29 June 2024; Accepted 4 July 2024
Available online 14 July 2024

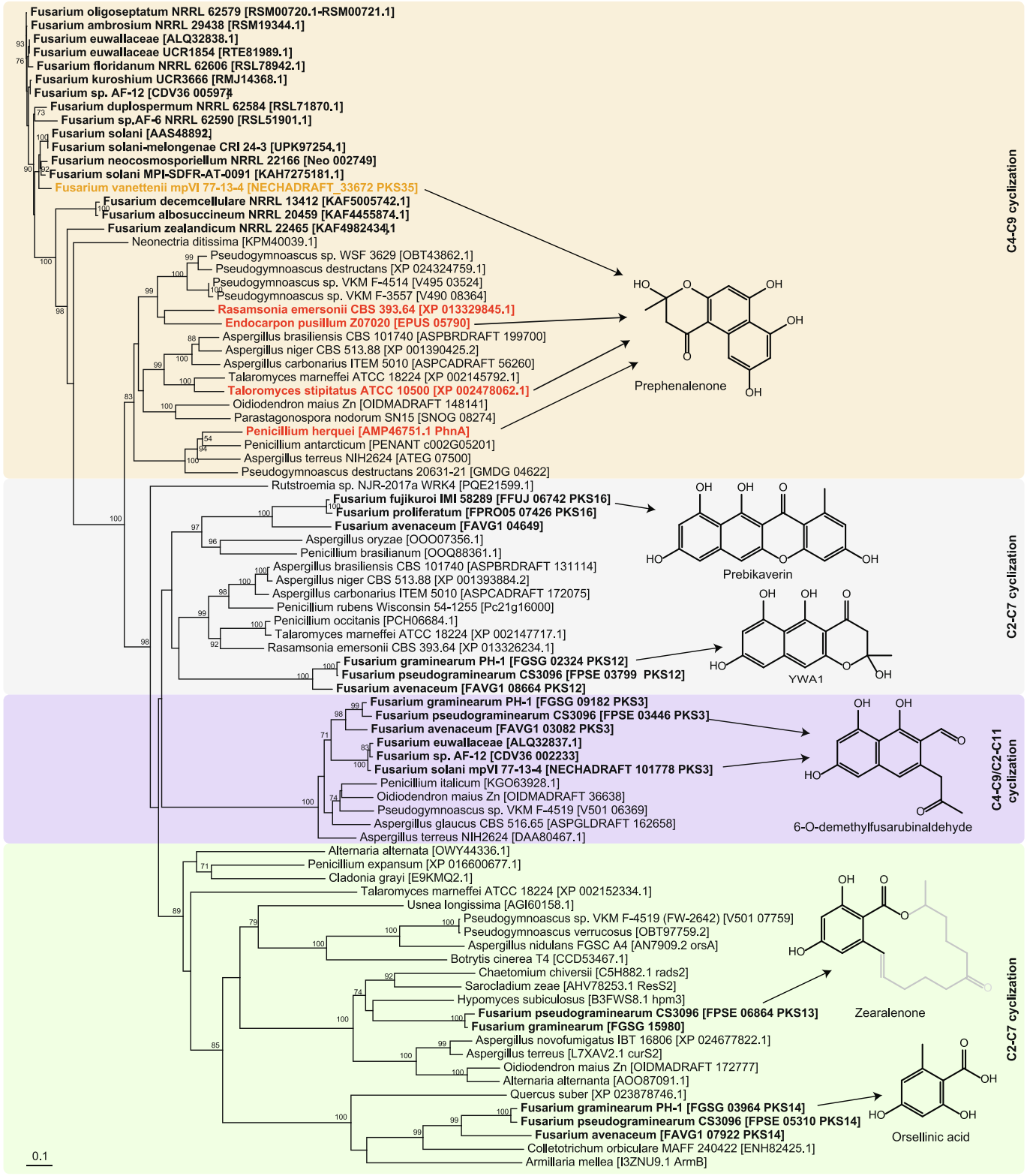

Fig. 1. Phylogenetic tree obtained by maximum likelihood analyses of PT domains from non-reducing PKSs from *Fusarium* (bold) and selected PKSs from GenBank. Initial PKS chemical products are indicated. Bootstrap support (>70) from 100 replications are included at internal nodes. The *F. vanettenii* FsnI (PKS35) PT domain is highlighted in yellow. The PKS35 gene clusters from the fungi highlighted in red, along with the *F. vanettenii* PKS35 cluster, were compared by synteny plot. The aldol condensation reaction directed by different PT domains are indicated on the right and are grouped by color.

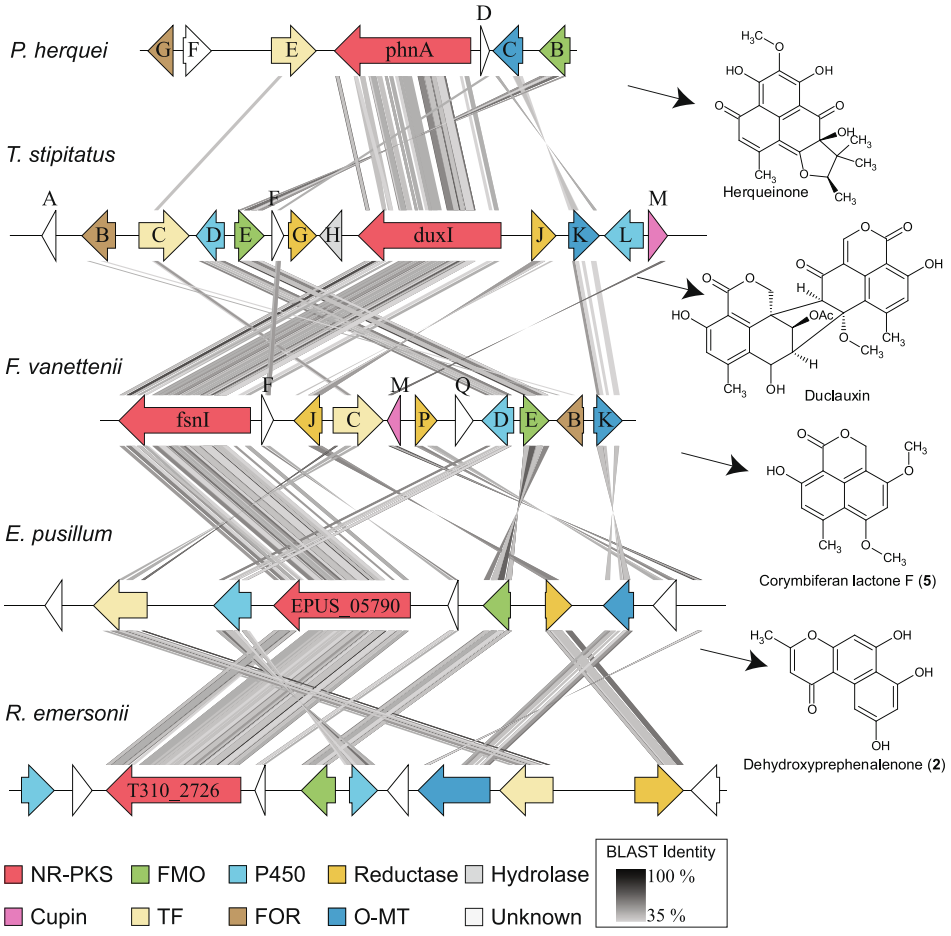

Fig. 2. Synteny plot comparison of *F. vanettenii* 77–13-4 PKS35 gene cluster to putative orthologous gene clusters from other fungi. BLAST identity is shown as grey to black bars between putative gene homologs. The chemical product of the *P. herquei phn* cluster is herqueinone and the chemical product of the *T. stipitatus dux* cluster is duclauxin. The possible product of the *F. vanettenii PKS35* cluster is corymbiferan lactone F (this work). The chemical product of the *E. pusillum* PKS encoded by EPUS_05790 is prephenalenone. The chemical product of the *R. emersonii* PKS T310_2726 gene cluster is unknown.

pigment is the ancestral state of the genus (Brown et al., 2022).

The predicted domain architecture of pigment-producing PKSs is similar and consist of a starter unit acyltransferase (SAT), a ketosynthase (KS), acyltransferase (AT), a product template (PT) domain, two acyl carrier protein (ACP) domains and a thio-esterase / claisen cyclase (TE) domain (Graziani et al., 2004; Hansen et al., 2015; Hansen et al., 2012). Phylogenetic analysis indicate that PKS35 is a possible orthologue of PhnA from *Penicillium herquei*, which produces the heptaketide prephenalenone (Gao et al., 2016). The rare angular structure of prephenalenone is facilitated by the PKSs unique PT domain that catalyze a C4 – C9 aldol condensation reaction. The transformation of prephenalenone to phenalenone is catalyzed by the FAD-dependent monooxygenase (FMO) PhnB, which is responsible for simultaneous C2 aromatic hydroxylation and opening of the γ-pyrone ring (Gao et al., 2016).

A major challenge to determining the structure of perithecial pigments in FSSC is the difficulty in obtaining sufficient material for chemical structure studies. Perithecial development span a few weeks or more and does not yield an abundance of tissue per agar plate. One strategy to increase fungal chemical synthesis is to express a cluster specific transcription factor that then expresses the clusters biosynthetic genes. This approach successfully linked several polyketide-derived chemicals to their responsible gene clusters in *Fusarium* including bostrycoidins and fusarielins in *F. graminearum* (Sørensen et al., 2012; (Frandsen et al., 2016), equisetin in *F. heterosporum* (Kakule et al., 2013) and fujikurins in *F. fujikuroi* (Von Bargen et al., 2013). A second challenge is the lack of convenient fungal genetic tools in FSSC. This was recently overcome using yeast recombinational cloning to assemble fungal vectors and *Agrobacterium tumefaciens* to transform vectors into the fungus (Nielsen et al., 2019a; Nielsen et al., 2022). In this study, we employed the described methodologies in conjunction with both heterologous and homologous gene expression techniques to elucidate the principal chemical compound generated by the *PKS35* gene cluster.

2. Material and methods

A list of all primers used in this study can be found in Supplementary Table 1. A list of plasmids created and utilized in this study can be found in Supplementary Table 2. The PKS35 cluster genes are listed in Supplementary Table 3 together with predicted functions. All mutant strains produced in this study are listed in Supplementary Table 4.

2.1. Strains and media

Fusarium vanettenii 77–13-4 (FGSC 9596, NRRL45880, synonym *Fusarium solani* f. sp. *pisi*, previously *Nectria haematococca* mp VI) and *Fusarium graminearum* PH-1 (NRRL31084) were maintained on Czapek Dox (Cz) or potato dextrose agar (PDA) with supplements (Frisvad, 2012). *F. vanettenii* transformants were maintained on media supplemented with 150 μg/mL geneticin G418 or 120 μg/mL hygromycin B when applicable. *F. graminearum* transformants were maintained on media supplemented with 300 μg/mL G418. For production of

metabolites, fungal strains were cultivated on yeast extract sucrose (YES) (Sørensen and Sondergaard, 2014) or Defined Fusarium medium (DFM) (Malz et al., 2005).

Saccharomyces cerevisiae BY4743 (Euroscarf Y20000), used for plasmid assembly, was maintained on YEPD (0.3 % yeast extract, 1 % peptone, 2 % glucose, X% agar). For selection of transformants and for maintaining heterologous expression vectors, yeast synthetic drop-out medium without uracil (SC-U; Sigma Y1501), without leucine (SC-L; Sigma Y1376), or without uracil and leucine (SC-UL; Sigma Y2001, added 76 mg/L histidine and 76 mg/L tryptophane) was prepared with yeast nitrogen base without amino acids (Sigma Y0626) and 2 % glucose according to manufacturer's specifications. *Escherichia coli* DH5α, used for yeast-plasmid recovery and propagation, was grown on solid (2 % agar) or liquid Luria-Bertani (LB, Lennox) medium supplemented with 50 μg/mL kanamycin at 37 °C when applicable. *Agrobacterium tumefaciens* AGL-1, used for transformation of *F. vanettenii*, was grown on yeast malt agar medium (Oxoid, CM920) supplemented with 10 μg/mL rifampicin, 100 μg/mL streptomycin or 50 μg/mL kanamycin when applicable.

2.2. Bioinformatic analyses

Amino acid sequences of predicted PT domains from non-reducing PKSs from *Fusarium* and closely related species were retrieved from GenBank (http://www.ncbi.nlm.nih.gov) essentially as described (Jørgensen et al., 2014). The sequences were aligned and analyzed in CLC Genomics Workbench (Qiagen, Hilden, Germany) using default parameters. The evolutionary history of the PT domains within and among species was then inferred using maximum likelihood analysis. Statistical support for branches were generated by bootstrap analysis with 1000 bootstraps (Severinsen et al., 2023).

To explore the breadth of the PKS35 gene cluster in *F. vanettenii*, predicted genes neighboring PKS35 (*fsnI*) (NECHADRAFT_33672) were investigated using CD-Search (https://www.ncbi.nlm.nih.gov/Structure/cdd/cdd.shtml).

Shared synteny of the putative *F. vanettenii PKS35* gene cluster (*fsnIFJCMPQDEBK*) was investigated by comparing it to possible orthologous clusters from *Rasamsonia emersonii* CBS 393.64 (T310_2724-2733, PRJNA292605), *Penicillium herquei* NRRL20711 (*phnABCDEFG*, gene_12204-12211, (Petersen et al., 2023)), *Talaromyces stipitatus* NRRL10500 (*duxABCDEFGHIJKLM,* TSTA_083230-083350 (Gao et al., 2018)), *Endocarpon pusillum* Z07020 (EPUS_05787-05795 (Harvey et al., 2018)). Linear comparison figures of the multiple genomic loci were generated with Easyfig v. 2.1 (Sullivan et al., 2011) as described in (Nielsen et al., 2019a) (Fig. 2).

Genomic sequence flanking *PKS35* homologs was retrieved from 28 publicly available *Fusarium* genomes including *F. vanettenii* 77–13-4 (Coleman et al., 2009), *F. solani* FSSC 5 MPI-SDFR-AT-0091 (Mesny et al., 2021), *F. ambrosium* NRRL20438, *F. floridanum* NRRL62606, *F. kuroshium* UCR3641, *F.* sp. AF-6 NRRL62590, *F. duplospermum* NRRL62584, *F. oligoseptatum* NRRL62579, *F. euwallaceae* NRRL62626 UCR1854 (J.E. Stajich et al., unpublished), *F. euwallaceae* HFE-W_16_IV_019 (Ibarra-Laclette et al., 2017), *F. solani-melongenae* (Xie et al., 2022), *F. neocosmosporiellum* NRRL22166 (Kim et al., 2019), *F. neocosmosporiellum* NRRL22436, *F. cicatricum* NRRL54954 (Brown et al., 2022), *F. liriodendri* NRRL22389 (H.-S. Kim, 2022, unpublished), *F. devonianum* NRRL22134, *F. staphyleae* NRRL22316 (R. H. Proctor & H.-S. Kim, 2021, unpublished), *F. dimerum* NRRL20691, *F. penzigii* NRRL20711, *F. domesticum* NRRL29976, *F. robinianum* NRRL25729, *F. zealandicum* NRRL22465, *F. decemcellulare* NRRL13412, *F. albosuccineum* NRRL20459, *F. setosum* NRRL36526, *F. drepaniforme* NRRL62941, *F. tuaranense* NRRL46518 (H.-S. Kim et al. 2020), and *F. cyanostomum* NRRL53998 (C.E. Probyn et al. 2020, unpublished) and compared using Easyfig as above. The 28 species are members of six different species complexes including Solani (16), Staphyleae (4), Dimerum (3), Decemcellulare (3), Buxicola (1) and Ventricosum (1). PKS35 from *Neonectria ditissima* R09/05 (Gómez-Cortecero et al., 2015) was used to illustrate the conserved region.

Phylogenetic analysis of *PKS35* and *PKS3* cluster transcription factor genes and selected other transcription factor genes were conducted on nucleotide sequences of predicted open reading frames (ORFs) retrieved from GenBank in MEGA-X (Tamura et al., 2021).

2.3. Heterologous expression of F. Vanettenii fsnI and fsnE in Saccharomyces cerevisiae

The *F. vanettenii fsnI* ORF was cloned by amplifying the six predicted exons using primers containing 15 bp tails homologous to the adjacent exon (Supplementary Table 1). The outermost primers A057 and A079 contained 30 bp tails homologous to the insertion site of the yeast expression vector pYES2 (Invitrogen). A *fsnI* expression vector was constructed using target associated recombination (TAR)-mediated cloning as previously described (Bejenari et al., 2023; Pedersen et al., 2020). The vector was co-transformed into *S. cerevisiae* with a vector containing a gene encoding a 4′-phosphopantetheinyl transferase from *F. verticillioides* (*FvPPT1*) that was codon-optimized for yeast (Pedersen et al., 2022). Yeast transformant *Sc* O-*PPT* O-*fsnI* was grown under galactose inducing conditions (Pedersen et al., 2020) and metabolites were extracted from pelleted cells with 5 mL ethyl acetate:dichloromethane:methanol (3:2:1) solution plus 1 % (v/v) formic acid in an ultrasonic bath for 60 min. The organic phase was evaporated under a flow of N_2 gas and the resulting material was dissolved in 800 μL methanol. Insoluble materials were removed by filtration with a 0.45 μm syringe filter.

A yeast codon-optimized version of *fsnE* (NECHADRAFT_76234), encoding a putative FAD-dependent monooxygenase, was synthesized by GenScript Biotech, amplified with primers E032/E033, and cloned into the pESC-LEU:*PPT* linearized with *Bgl*II and *Not*I. The resulting construct pESC-LEU:*PPT*:*fsnE* was validated by Sanger sequencing with primers E034 and E043. pESC-LEU:*PPT*:*fsnE* was then transformed into *S. cerevisiae* together with pYES2:*fsnI* and grown under inducing galactose conditions for five days prior to extraction.

2.4. Genetic manipulation of Fusarium vanettenii

Gene overexpression and gene deletion experiments were carried out as previously described (Nielsen et al., 2022). In brief, *F. vanettenii* conidia were transformed using *Agrobacterium tumefaciens* plasmids tailored to either delete a target gene by double homologous integration or overexpress a gene by ectopic integration of the transforming DNA. To create the cluster overexpression vector, the predicted cluster transcription factor *fsnC* was first amplified from *F. vanettenii* genomic DNA using primers OE_fsnC_Fwd /OE_fsnC_Rev and fused with the constitutive *TEF-1α* promoter using TAR cloning, resulting in plasmid pSHUT4:*fsnC* following *Bam*HI/*Xho*I digestion of pSHUT4-eYFP (Addgene 133094). Single-colony TAR constructs were recovered and proliferated in *E. coli* before PCR screening with primers E022/E023. *A. tumefaciens* AGL-1 pSHUT4:*fsnC* was used to transform *F. vanettenii* conidia using G418 (Gibco) for selection (Nielsen et al., 2022), whereafter the resulting *Fv* OE::*fsnC* transformants were screened by PCR using primers D096/C091 and D096/D097 testing correct recombination between T-DNA and the β-tubulin locus.

The *fsnI* deletion plasmid was prepared by amplifying genomic DNA upstream and downstream of *fsnI* using primer sets KO_fsnI_UpFwd/KO_fsnI_UpRev and KO_fsnI_DwFwd/KO_fsnI_DwRev, respectively. The PCR products were then assembled with the *hph* selection marker from pRF-HU2 (Frandsen et al., 2008) and the plasmid backbone of pSHUT3-32 (Nielsen et al., 2019b) creating pKO-FSNI. Validation of the correct four-fragment DNA product was carried out by PCR on plasmid isolated from single yeast colonies with primers C090/G058 and G059/C093. Finally, transformation of *F. vanettenii* wild-type and mutant *Fv* OE::*fsnC* strains was carried out as above yielding mutant *Fv* Δ*fsnI* and double

mutant *Fv* OE::*fsnC* Δ*fsnI*. Deletion of *fsnI* was analyzed by PCR with primers G056/G057, locus_fsnI_Fwd/G058, and G059/locus_fsnI_Rev, and G062/G063 as a negative control. The PKS3 (*fsr1*) deletion plasmid, available from a previous study (Nielsen et al., 2022), was used to transform strain *Fv* OE::*fsnC* yielding the double mutant *Fv* OE::*fsnC* Δ*fsr1*. Deletion *fsr1* was analyzed by PCR with primers G056/G057, locus_fsr1_Fwd/G058, and G059/locus_fsr1_Rev.

Following PCR validation, selected mutants were subjected to whole genome sequencing to confirm correct integration of vector DNA in targeted loci. High quality DNA for sequencing was isolated from mycelia harvested after five days growth in liquid YES media at 25 °C at 150 rpm, using the phenol–chloroform method described in (Petersen et al., 2022). Minimap2 version 2.17 (Li, 2018) was used to map the reads to *in silico* generated chromosome 2 and 10 retrieved from GenBank accensions GG698910 and GG698970 for *F. vanettenii* (Figures S2, S3, S5 and S6) (Coleman et al., 2009).

2.5. Reconstruction of the PKS35 gene cluster in Fusarium graminearum

To verify the findings from the ectopic overexpression analyses, the entire PKS35 gene cluster was cloned and transformed into *F. graminearum* for heterologous expression, essentially as described (Nielsen et al., 2019b); (Nielsen and Sørensen, 2022). Plasmids pS33501 and pS33502, each containing the 11 gene PKS35 cluster, were transformed into *F. graminearum* using the protoplast method as previously (Twaruschek et al., 2018). G418-resistant transformants were screened for correct integration at the β-Tubulin locus by PCR with primers flanking the target integration site FgTUB-Fw/nptII-Rv and $pTAR_9$-Fw/FgTUB-Rv. Two PCR positive strains were genome sequenced by DNAsense (Aalborg, Denmark) to verify that the intact *PKS35* gene cluster had been inserted into the *F. graminearum* genome.

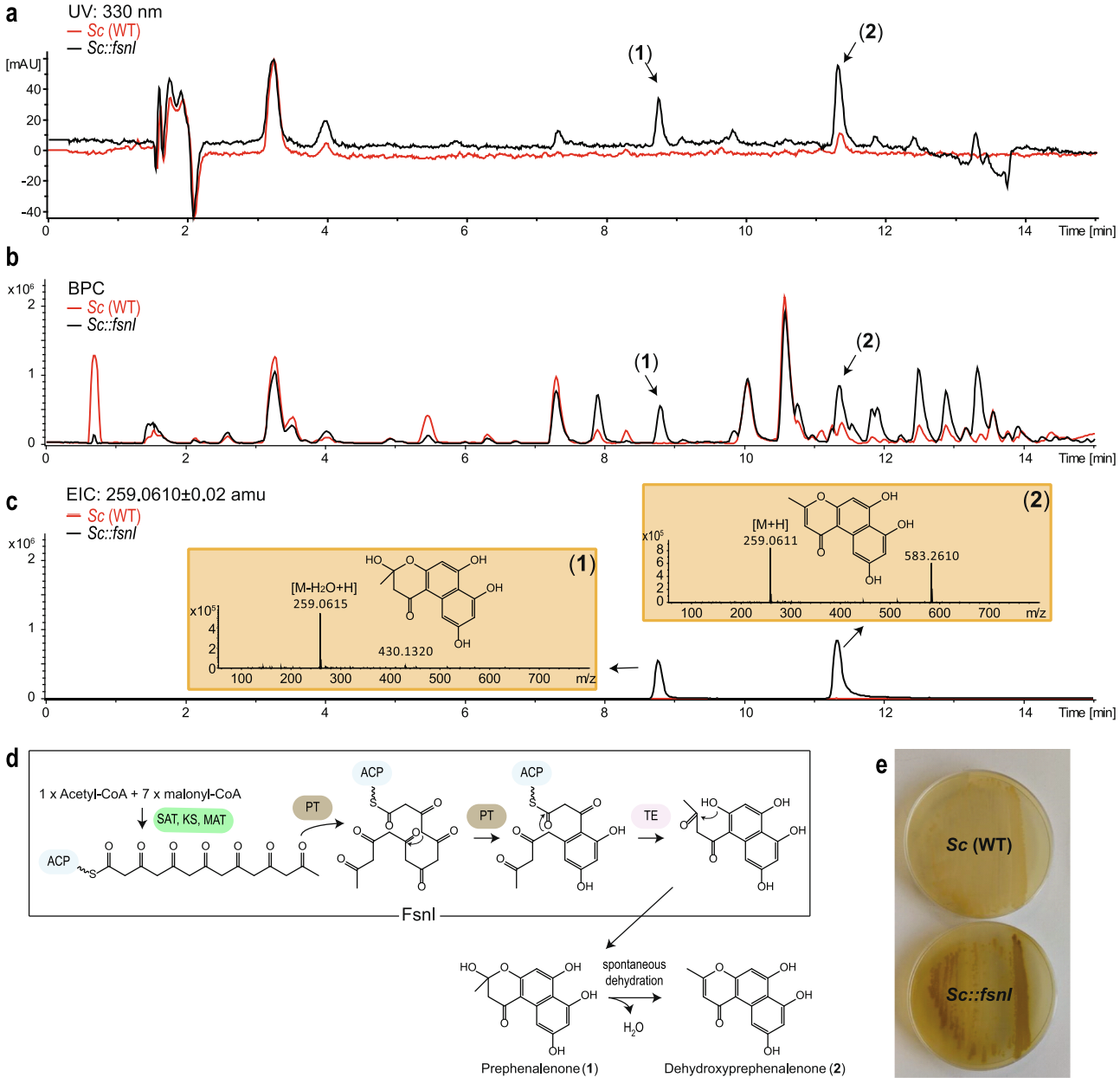

Fig. 3. HPLC-MS analysis of *S. cerevisiae* wild-type and mutant strain expressing *fsnI* and *FvPPT1*. UV chromatogram at 330 nm (**A**), Base peak chromatogram (**B**) and extracted ion chromatogram (**C**) at 259.0610 ± 0.02 amu. **D.** Proposed biosynthesis of prephenalenone (1) and formation of dehydroxyprephenalenone (2). **E.** Photograph of *S. cerevisiae* wild type and heterologous expression strain showing formation of pigmented colonies.

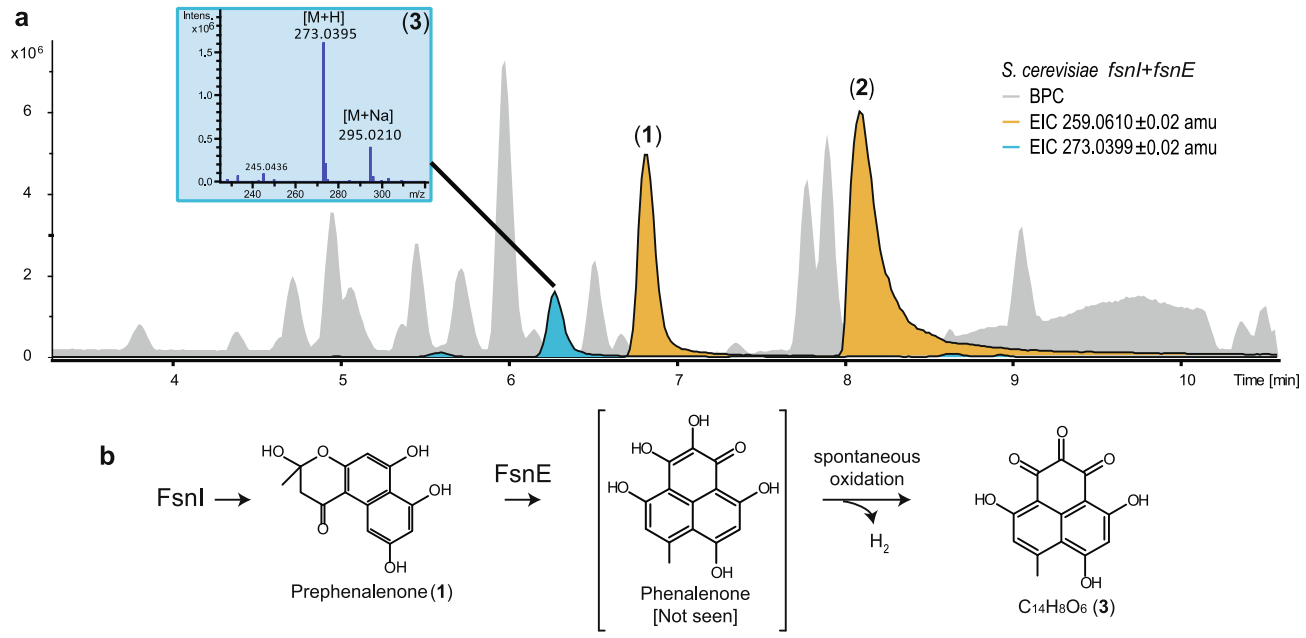

Fig. 4. HPLC-MS analysis of *S. cerevisiae* mutant strain expressing PKS *fsnI* and monooxygenase *fsnE*. The base peak chromatogram is shown in grey. An extracted ion chromatogram at 259.0610 ± 0.02 amu (orange) included two major peaks corresponding to prephenalenone (**1**, $[M-H_2O+H]^+$) and deoxyprephenalenone (**2**, $[M+H]^+$). An extracted ion chromatogram at 273.0399 ± 0.02 amu (blue) ($C_{14}H_8O_6$) included a one major peak that likely corresponding to **compound 3** ($[M+H]^+_{(theoretical)}$ = 273.03991 amu).

2.6. Chemical analyses

Transformants were grown as three point inoculated cultures on solid YES, PDA, YPD and Cz agar plates in triplicates for two weeks in the dark at 25 °C. Secondary metabolites were extracted from 10 plugs using the microscale extraction method with ethyl acetate:dichloromethane: methanol (3:2:1) plus 1 % (v/v) formic acid (Smedsgaard, 1997). The extracts were dissolved in 500 µL methanol and analyzed by reverse phase-high performance liquid chromatography coupled to a Bruker quadrupole time-of-flight (gTOF) high resolution mass spectrograph (RP-HPLC-HRMS), as previously described (Westphal et al., 2019; Wollenberg et al., 2017).

2.7. Isolation and structural characterization of corymbiferan lactone F

100 Cz agar plates inoculated with strain *Fv* OE::*fsnC* Δ*fsr1* were grown at 28 °C for 14 days prior to metabolite extraction. The agar media were diced using a sterile scalpel and extracted with 4 L of ethyl acetate:dichloromethane:methanol (3:2:1) plus 1 % (v/v) formic acid.

Preparative LC-MS was performed with a Waters AutoPurification System using a hexylphenyl-column (Waters XBridge Prep C6Ph OBD 19 x 250 mm, 5 µm granule size) at a flow rate of 20 mL/min. The gradient began at 60 % acetonitrile/40 % water for 1 min, then increased linearly to 99 % acetonitrile/1% water over 9 min, and remained constant for 2 min. Both water and acetonitrile (VWR, LC-MS grade) contained 0.1 % (v/v) formic acid (Sigma Aldrich, LC-MS grade). The signal of the QDa detector was used to trigger fraction collection. Fractions were dried *in vacuo* and redissolved in MeOH, centrifugated and the pellet was then dried and dissolved in DMSO-d_6.

NMR spectra were recorded on a Bruker AVIII-600 MHz spectrometer equipped with a cryogenically cooled triple resonance 5 mm probe with z-gradients controlled by TopSpin 3.5pl6 software (Severinsen et al., 2023; Westphal et al., 2019). All spectra were acquired at 308.1 K in DMSO-d_6 (99.9 atom % D, 0.03 % (v/v) TMS, Sigma-Aldrich) and calibrated to internal TMS ^{1}H and ^{13}C (0.0 ppm) signals. ^{1}H NMR, [^{1}H,^{13}C]-HSQC and a [^{1}H,^{13}C]-HMBC optimized for J_{CH} = 8 Hz were recorded for structure elucidation. The ^{13}C chemical shifts and their assignment were reviewed by the CSEARCH Robot Referee (Robien, 2017).

3. Results and discussion

3.1. Phylogenetic analysis of the PKS35 gene cluster

A comparative analysis of PKSs in the *Fusarium* genus showed that PKS35 homologs were present in 36 of 206 species examined which included 19 members of the FSSC, as well as members of six other species complexes (Brown et al., 2022) (**Figure S1**). A phylogenetic analysis was conducted of PT domains collected from representative PKS35 *Fusarium* orthologues, non-reducing PKSs from *Fusarium* and selected PKSs from GenBank to obtain structural information about the chemical product directed by *F. vanettenii* PKS35 (FsnI) predicted PT domain (e.g., linear or angular multicyclic polyketide) (Fig. 1). Consistent with previous results, the phylogenetic analysis identified FsnI as a likely orthologue of prephenalenone PKSs PhnA from *Penicillium herquei,* DuxI from *Talaromyces stipentatus* and EPUS_05790 from *E. pusillum* (Harvey et al., 2018). This cluster also contains a possible orthologue from *Aspergillus terreus* (ATEG_07500), which has not yet been linked to a product. The *Fusarium* orthologues included PKS35 genes from *F. solani* strain CBS 225.58 and PKS35 from *F. neocosmosporiellum* (NRRL22166), which when deleted resulted in albino perithecia (Graziani et al., 2004); (Kim et al., 2019). The closest relative to *PKS35* outside the *Fusarium* genus was identified in *Neonectria ditissima* R09/05 (KPM40039) which is a canker causing pathogen of fruit trees including apple and pear (Gómez-Cortecero et al., 2015). In another strain of *Neonectria*, five oxophenalenone pigments, neonectrolide A-E, were isolated, together with corymbiferan lactone E (Ren et al., 2015; Ren et al., 2012). It is unknown if this PKS35 ortholog and flanking genes are involved in neonectrolide synthesis in *Neonectria.*

A search of the Conserved Domain Database (CDD) at NCBI using CD-Search with nucleotide query sequences flanking *F. vanettenii fsnI* identified eight genes with predicted protein activities often associated with the synthesis of secondary metabolites. The eight proteins include a Zn $(II)_2Cys_6$ family transcription factor (*fsnC*), two alcohol dehydrogenases

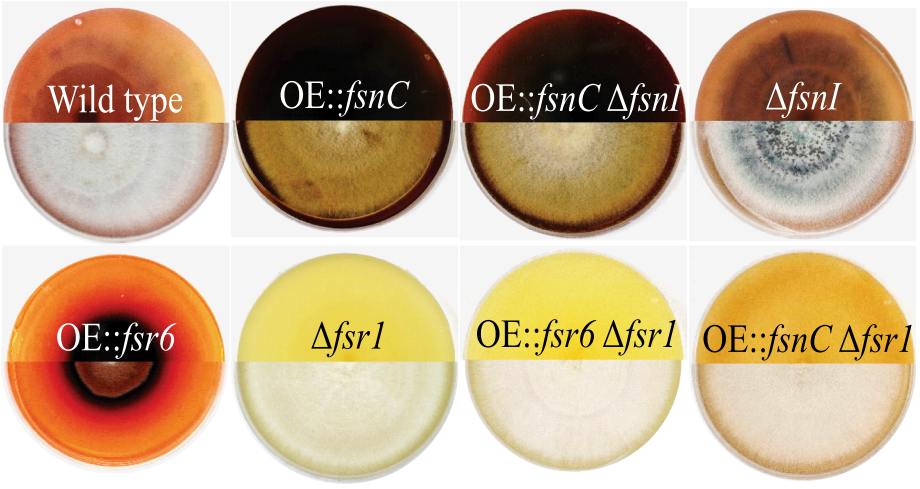

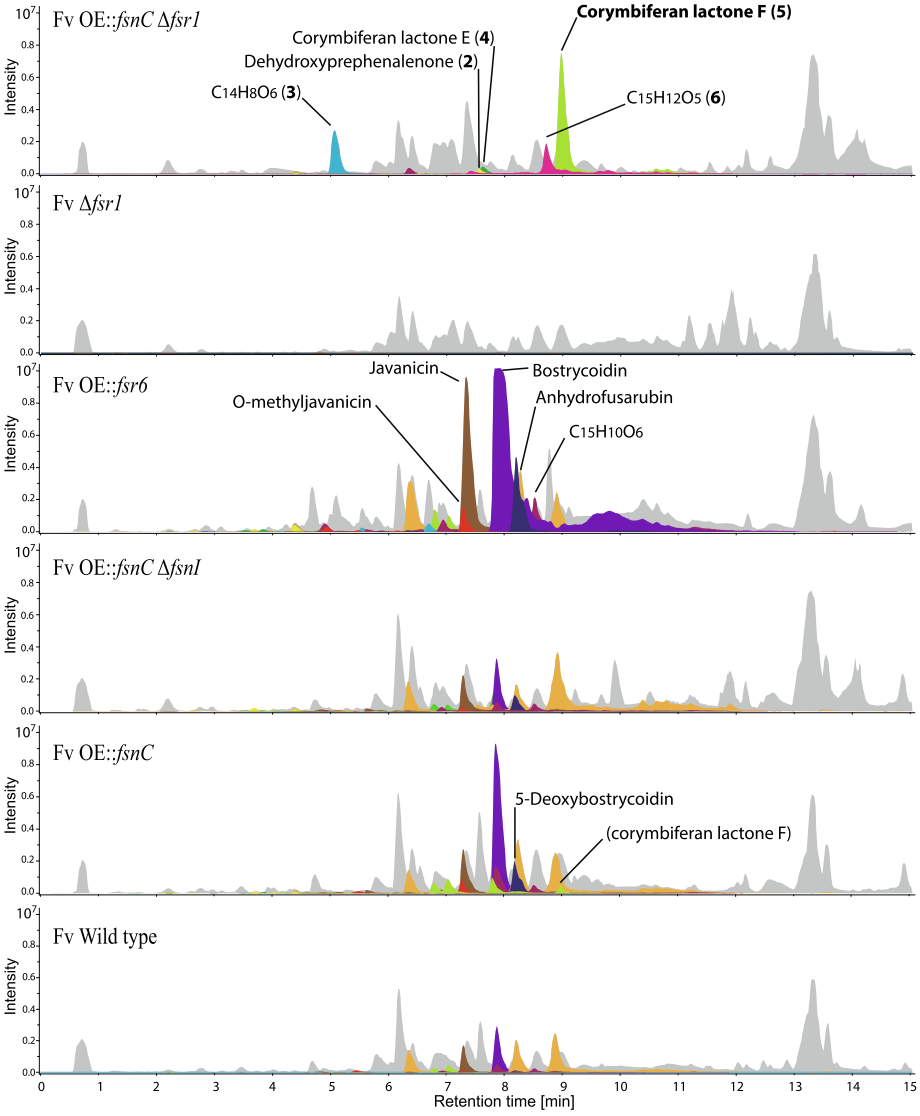

(caption on next page)

Fig. 5. **A**. *F. vanettenii* mutants and wild-type strain cultivated on Cz agar viewed from the top and the bottom of the petri dish. Wild-type, OE-*fsnC* = overexpression of transcription factor *fsnC*, OE-*fsnC* Δ*fsnI* = deletion of *fsnI* in OE-*fsnC*, Δ*fsnI* = deletion of *fsnI*, OE-*fsr6* = overexpression of transcription factor *fsr6*, Δ*fsr1* = deletion of *fsr1*, OE-*fsr6* Δ*fsr1* = overexpression of *fsr6* in Δ*fsr1* and OE-*fsnC* Δ*fsr1* = overexpression of *fsnC* in Δ*fsr1*. **B**. Base peak chromatograms (grey) and extracted ion chromatograms highlighting PKS3 (*fsr1*) and PKS35 (*fsnI*)-derived polyketide metabolites produced by mutant strains of *F. vanettenii*. Overexpression of transcription factor genes *fsnC* and *fsr6* led to production of dark/black/red mycelia and agar medium due to accumulation of PKS3-derived polyketides O-methyljavanicin (red, $[M + H]^+$=305.1025 ± 0.02 amu), Javanicin (brown, $[M + H]^+$= 291.08683 ± 0.02 amu), Bostrycoidin (purple, $[M + H]^+$= 286.0715 ± 0.02 amu), 5-deoxybostrycoidin (dark blue, $[M + H]^+$= 270.0766 ± 0.02 amu), Anhydrofusarubin (orange, $[M + H]^+$=289.0713 ± 0.02 amu), and a molecule deconvoluted to $C_{15}H_{10}O_6$ (dark red, $[M + H]^+$=287.0556 ± 0.02 amu). Loss of PKS35-derived polyketides (i.e., in deletion of *fsnI* in the *fsnC*-overexpression strain; OE-*fsnC* Δ*fsnI*) did not impact production of PKS3-derived polyketides. In contrast, deletion of the *fsr1* (PKS3, Δ*fsr1*) resulted in an albino phenotype with no detectable levels of PKS3-derived compounds. Deletion of *fsr1* in the *fsnC*-overexpression strain (OE-*fsnC* Δ*fsr1*) revealed novel masses putatively associated with the PKS35 gene cluster including: $C_{14}H_8O_6$ (**Compound 3**, blue, $[M + H]^+$= 273.0399 ± 0.02 amu), Dehydroxyprephenalenone (**Compound 2**, yellow, $[M + H]^+$= 259.0606 ± 0.02 amu), Corymbiferan lactone E (**Compound 4**, dark green, $[M + H]^+$= 261.0763 ± 0.02 amu), $C_{15}H_{12}O_5$ (**Compound 6**, pink, $[M + H]^+$= 273.0763 ± 0.02 amu), and Corymbiferan lactone F (**Compound 5**, light green, $[M + H]^+$= 275.0920 ± 0.02 amu). MS and UV spectra of PKS35-related compounds are shown in Supplementary Figure S7

(*fsnJ, fsnP*), two monooxygenases (*fsnD, fsnE*), an oxidoreductase (*fsnB*), an O-methyltransferase (*fsnK*), and a cupin dioxygenase (*fsnM*). Two other predicted ORFs (*fsnF*, *fsnQ*) did not share similarity with previously characterized genes (Supplementary Table 3).

We next constructed a synteny plot comparing the prephenalenone biosynthetic gene clusters from *Penicillium herquei, Talaromyces stipitatus*, *Endocaron pussilum* and *Rasamsonia emersonii* to the putative *F. vanettenii* PKS35 cluster (*fsnIFJCMPQDEBK*). We found that the 10 genes adjacent to *fsnI* in *F. vanettenii* share homology with four (*P. herquei*), eight (*T. stipitatus*), seven (*E. pusillum*) and six (*R. emersonii*) genes that flank the *fsnI* homologs in these respective fungi (Fig. 2). Finally, examination of the available *Fusarium* genome sequences showed that the 11 membered *PKS35* gene cluster is conserved in genomes of FSSC as well as six other *Fusarium* species complexes ((Brown et al., 2022; Pokhrel and Coleman, 2023); **Figure S1**).

3.2. Identification of the entry compound produced by FsnI

To identify the chemical product synthesized by FsnI, the predicted open reading frame was expressed in *Saccharomyces cerevisiae* under the control of an inducible GAL1 promoter (*Sc*::*fsnI*). After five days of cultivation under inducing conditions, the *Sc::fsnI* culture media was yellow and the subsequent extracts contained two peaks that were not present in extracts of the *S. cerevisiae* wild type (Fig. 3). The predominant ions for the two peaks in the HRMS spectrum were 259.0615 and 259.0611, which match well with prephenalenone (**compound 1**, $C_{14}H_{12}O_6$; $[M + H\text{-}H_2O]^+$: 259.0607) and a dehydrated product dehydroxyprephenalenone (**compound 2**, $C_{14}H_{10}O_5$; $[M + H]^+$: 259.0607). Both of these chemicals were detected after expression of orthologous PKSs in yeast from *Penicillium herquei*, *Talaromyces stipitatus* and *Endocarpon pusillum* (Gao et al., 2016; Gao et al., 2018; Harvey et al., 2018). This suggest that the biosynthetic route for the *F. vanettenii* perithecial pigment has an identical entry compound as the herqueinone pathway in *P. herquei* and the duclauxin pathway in *T. stipitatus*.

To determine the next step in the biosynthetic pathway, we coexpressed *fsnE*, which encodes a putative monooxygenase, with *fsnI*, in *S. cerevisiae* (*Sc*::*fsnI* + *fsnE*). *phnB* and *duxE*, putative homologs of *fsnE*, have been shown to catalyze the formation of phenalenone from prephenalenone (Gao et al., 2016; Gao et al., 2018). In addition to **1** and **2** in *Sc*::*fsnI* + *fsnE*, extracts contained a new peak **(3)** with a mass of 273.0395 $[M + H]^+$ (Fig. 4). The molecular formula that corresponds well with this mass is $C_{14}H_8O_6$ (theoretical $[M + H]^+$: 273.03991) which has been reported to be a spontaneous oxidation product of phenalenone (Gao et al., 2016). We did not detect a mass consistent with phenalenone in our *S. cerevisiae* expression experiments.

3.3. Activation of the PKS35 cluster transcription factor in F. Vanettenii leads to formation of PKS3- and PKS35-derived polyketides

To activate expression of all *PKS35* cluster genes in *F. vanettenii*, we overexpressed the predicted cluster transcription factor *fsnC* using the constitutive TEF-1α promoter. The expression cassette was transformed into *F. vanettenii* by ATMT and yielded 6 transformants. Three transformants were positive by colony PCR for the transforming DNA of which one, referred to here after as *Fv* OE::*fsnC*, was whole genome sequenced to verify the presence of the expression cassette (**Figure S2**). *Fv* OE::*fsnC* was grown on agar plates and in liquid media for two weeks prior to chemical analysis of culture extracts. Over this time, the agar media developed a deep red color, which contrasted with the lighter red/pale color of wild type cultures (Fig. 5). The secondary metabolite profile revealed the presence of anhydrofusarubin, bostrycoidin and javanicin which are products derived from PKS3 (*fsr1*) as well as corymbiferan lactone F. An extract from *Fv* OE::*fsnC* grown on solid Cz media contained O-methyljavanicin and 5′-deoxybostrycoidin, which were not detected in extracts of the wild-type parent. This overproduction of *fsr1*-derived compounds by *Fv* OE::*fsnC* mirrored that of the *fsr6* overexpression strain, *Fv* OE::*fsr6* except for no corymbiferan lactone F was detected (Nielsen et al., 2019a).

We were intrigued to find that forced expression of the *fsnC* led to an increase in production of another PKS cluster chemical. We therefore deleted *fsr1* (**Figure S3**), which is well known for biosynthesis of fusarubins and derivatives in *F. vanettenii* and other Fusaria (Nielsen et al., 2022). The observations that deletion of *fsnI* did not alter the appearance of mycelium significantly and that the media color of *Fv* OE::*fsnC* was similar to the double mutant *Fv* OE::*fsnC*-Δ*fsnI*, suggest that the PKS encoded by *fsnI* is not responsible for the dark color observed after forced expression of *fsnC* (**Figure S4**).

To further reveal the chemicals produced by the *PKS35* cluster, we deleted *fsr1* in the wildtype and *Fv* OE::*fsnC* mutant, which were validated by genome sequencing (**Figure S5 and S6**). Strain *Fv* Δ*fsr1*

Table 1
NMR result; the chemical shifts and HMBC correlations of Corymbiferan lactone F shown in Fig. 7.

Atom #	δ (^{13}C) [ppm]	δ (^{1}H) [ppm]	$^{n}J_{CH}$ (δ-^{13}C), observeable HMBC cross peaks to ^{13}C atoms with a chemical shift [ppm] of
1	169.32	–	–
2	96.12	–	–
3	161.74	–	–
3-OH	–	11.83	96.12, 117.39, 161.74
4	117.39	6.78 (d, *J* = 0.9 Hz)	24.96, 96.12
5	146.74	–	–
6	112.00	–	–
7	153.92	–	–
8	92.88	6.77 (s)	100.57, 112.00, 153.92, 159.07
9	159.07	–	–
10	100.57	–	–
11	66.42	5.62 (s)	100.57, 131.35, 153.92, 169.32
12	131.35	–	
13	24.96	2.76 (d, *J* = 0.9 Hz)	112.0, 117.39, 146.74
14	55.94	3.965 (s)	153.92
15	55.94	3.963 (s)	159.07

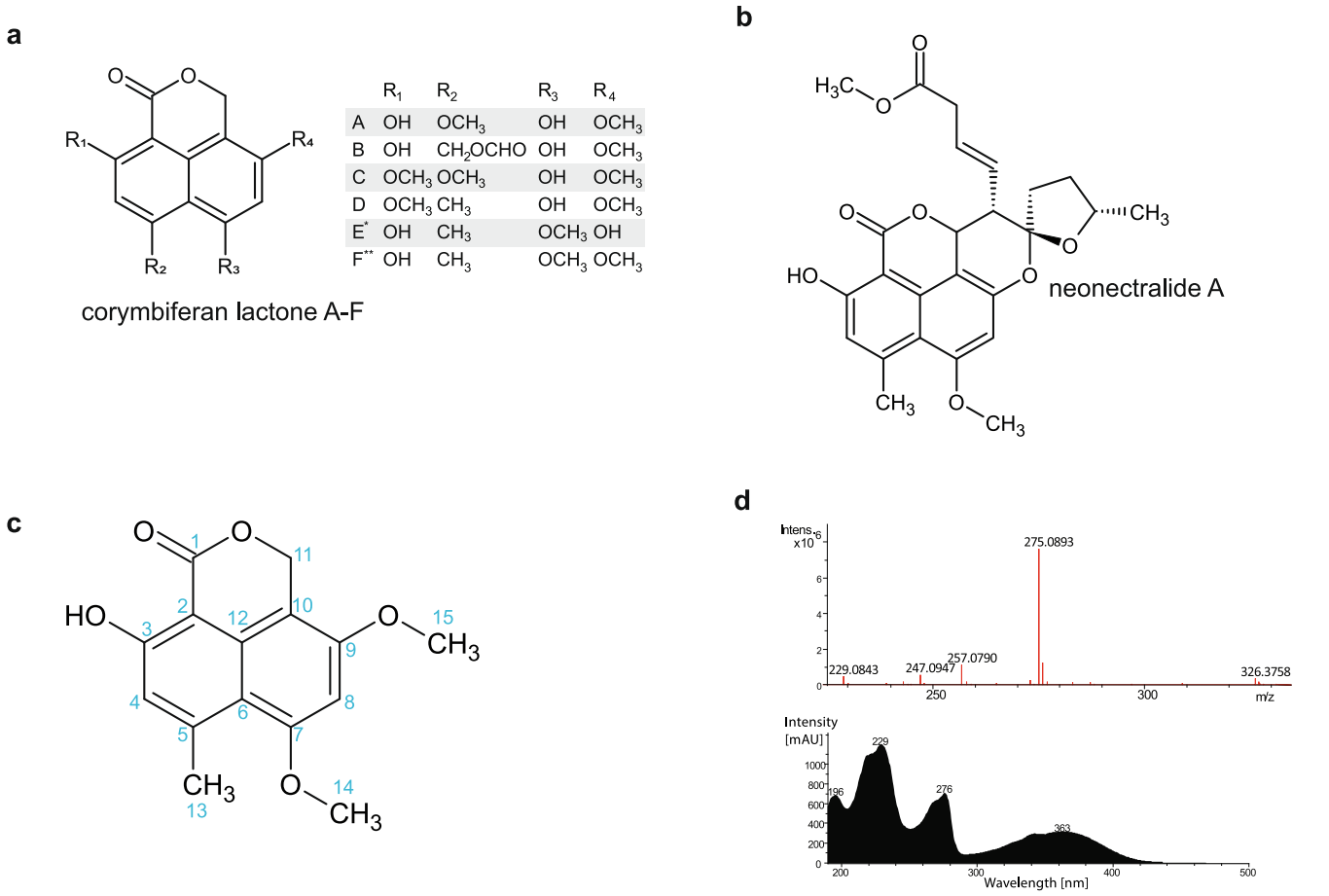

	R_1	R_2	R_3	R_4
A	OH	OCH_3	OH	OCH_3
B	OH	CH_2OCHO	OH	OCH_3
C	OCH_3	OCH_3	OH	OCH_3
D	OCH_3	CH_3	OH	OCH_3
E*	OH	CH_3	OCH_3	OH
F**	OH	CH_3	OCH_3	OCH_3

Fig. 6. Oxo-phenalenone polyketides produced by filamentous fungi. *Compound 4, **Compound 5. A) Corymbiferan lactones A-D isolated from Penicillium hordei [Overy 2004], corymbiferan lactone E from Neonectria sp. (Ren et al. 2015), corymbiferan lactone F isolated from F. vanettenii (this study). B) neonectralide A from Neonectria sp. (Ren et al. 2012). C) Chemical structure of corymbiferan lactone F shown with the atom numbering used throughout the article. D) HRMS and UV spectra of preparative LC fraction collected from Fv OE::fsnC Δfsr1 culture extract. The chemical shifts and HMBC correlations are given in Table 1.

produced pale or colorless mycelium while strain *Fv* OE::*fsnC*Δ*fsr1* produced yellow/orange mycelium. Analysis of extracts of *Fv* OE::*fsnC*Δ*fsr1* cultures contained compounds **2** and **3** (Fig. 5 and **Figure S7**), which were also observed when *fsnI* and *fsnE* were expressed in *S. cerevisiae*. The *Fv* OE::*fsnC*Δ*fsr1* extract chromatogram contained two additional peaks which are likely two different corymbiferan lactones. The first peak (compound **4**) had a mass of 261.0754 $[M + H]^+$ which corresponds to $C_{14}H_{12}O_5$ (theoretical: 261.0757 *m/z*) and is consistent with corymbiferan lactone E. This compound was originally isolated from a *Neonectria* species together with several other phenalenones (Ren et al., 2012). The second peak (compound **5**) was much more abundant and had a mass of 275.0906 $[M + H]^+$ which corresponded to $C_{15}H_{14}O_5$ (theoretical 275.0914 *m/z*). NMR analysis of purified **5** (Table 1 and Fig. 6, **S8, S9, S10 and S11**) led to its structural identification as a novel corymbiferan which we named corymbiferan lactone F. Corymbiferan lactone F differs from corymbiferan lactone E in that it has a methyl group at R_4.

This observed crosstalk between *PKS3* and *PKS35* could potentially occur through direct activation of the *PKS3* cluster genes by FsnC due to shared homology with Fsr6. To explore this possibility, we conducted a phylogenetic analysis of *fsnC* and *fsr6* putative homologs (**Figure S12**). The *fsnC* and *fsr6* homologs, including *pglR* (Frandsen et al., 2016), formed distinct clades. This suggest that the two transcription factors are not evolutionarily related and thus are not likely structurally similar and that the cross-activation by *fsnC* is not by direct induction of *fsr* gene transcription.

3.4. Heterologous expression of PKS35 cluster in Fusarium graminearum

To further verify that the *PKS35* cluster is responsible for biosynthesis of the phenalenones, we inserted the entire cluster at the β-Tubulin locus in *F. graminearum*. The cluster was amplified as eight overlapping PCR fragments and assembled in *S. cerevisiae* by yeast recombinational cloning (**Figure S13**). Transformation of *F. graminearum* with the vector containing the 11-gene cluster resulted in nine G418-resistant transformants. Putative transformants were screened by colony PCR with primers specific to two genes located inside the gene cluster. Two PCR positive transformants, *Fg35-14* and *Fg35-24*, were chosen for whole genome sequence analyses which showed that the *PKS35* gene cluster had integrated at the β-tubulin locus (**Figure S14**). *Fg35-14* also contained additional insertion events elsewhere on the genome. Both transformants and the parent wild-type strain were grown on solid YES medium for two weeks prior to extraction and analysis by HPLC-HRMS (Fig. 7). Chromatograms of *Fg35-14* extracts contained peaks corresponding to prephenalenone as well as compounds **2**–**5**, identified previously in *F. vanettenii fsnC* overexpression mutants, thus verifying that they are products of the *PKS35* cluster. All four compounds were also present in cultures extracts of *Fg35-24*, although at much lesser quantity, which could be due to a greater expression of the *PKS35* cluster genes due to the presence of multiple copies of the transforming DNA in *Fg35-14*. We also observed three additional peaks with similar UV spectra to compounds **2**–**5** but unique masses, in the chromatograms of both transformants (Fig. 7 and **Figure S15**). The extracted ion chromatograms of **2** and **5** resulted in

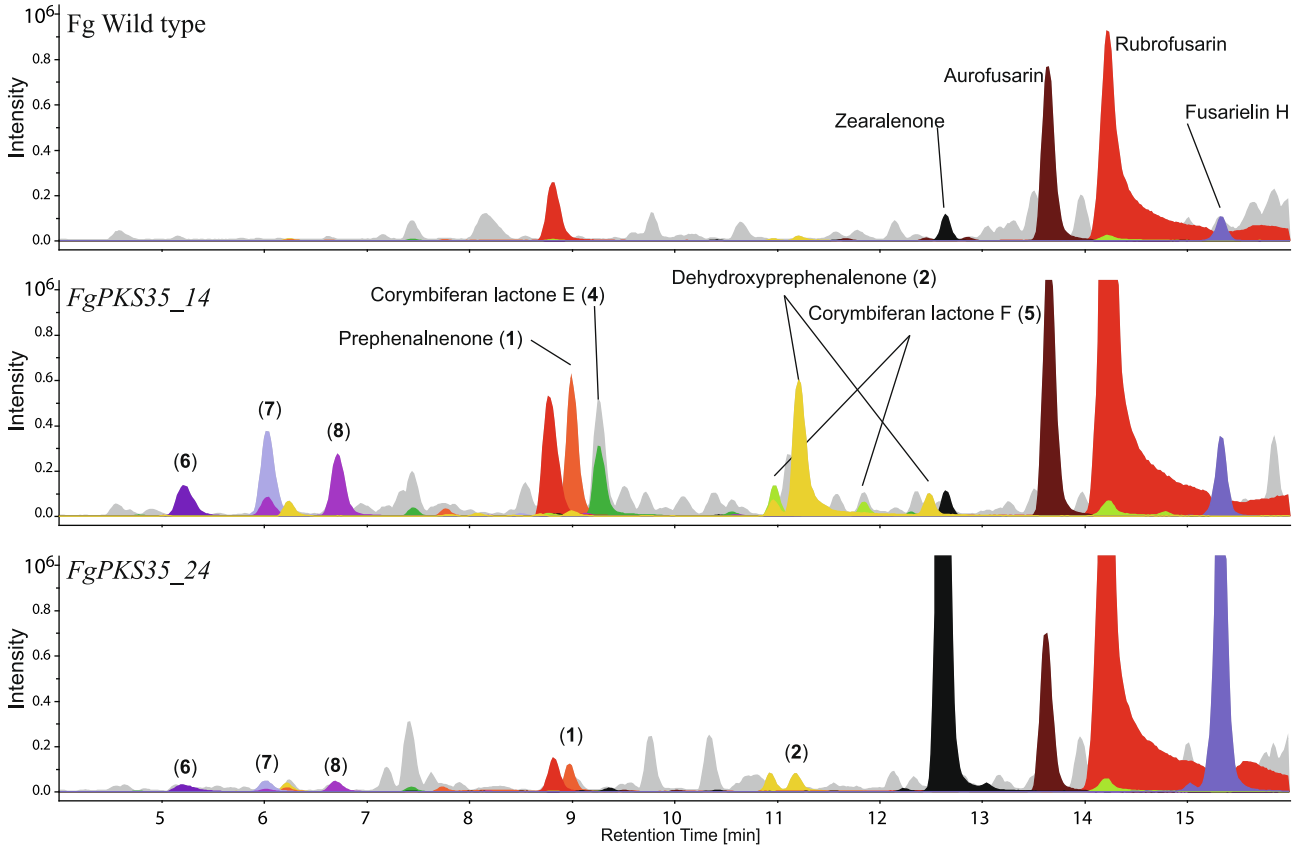

Fig. 7. Base peak chromatogram (grey) for the two *F. graminearum* strains (Fg35-14 and Fg35-24) heterologously expressing the PKS35 gene cluster and the parent wild type strain. Extracted Ion Chromatograms of known *Fusarium* metabolites present in both wild type and mutant extracts: 319.1545 ± 0.02 amu is Zearalenone $[M + H]^+$ (black), 571.0887 ± 0.02 amu is Aurofusarin $[M + H]^+$ (dark red), 273.0763 ± 0.02 amu is Rubrofusarin $[M + H]^+$ (red), and 369.2794 ± 0.02 amu is Fusarielin H $[M-H_2O + H]^+$ (blue). Both transformants were able to synthesize compounds with the same mass and UV spectra as compounds produced by the *F. vanettenii fsnC*-overexpression mutants: 277.0712 ± 0.02 amu is Prephenalenone (**Compound 1**) $[M + H]^+$ (orange), 261.0763 ± 0.02 amu is Corymbiferan lactone E (**Compound 4**) $[M + H]^+$ (dark green), 259.0606 ± 0.02 amu is Dehydroxyprephenalenone (**Compound 2**) $[M + H]^+$ (yellow), and 275.0920 ± 0.02 amu is Corymbiferan lactone F (**Compound 5**) $[M + H]^+$ (light green). Additionally, we observed three peaks, that were not previously observed in our *S. cerevisiae* and *F. vanettenii* experiments, which were deconvoluted to the elemental formulas: $C_{22}H_{26}NO_7$ (**Compound 6**, dark purple), $C_{19}H_{20}N_2O_7$ (**Compound 7**, light purple), and $C_{19}H_{19}NO_8$ (**Compound 8**, Purple). Select mass and UV spectra of observed peaks are shown in Supplementary Figure S11

two additional peaks, which could originate from compounds with identical elemental composition as an isomer of 2 has previously been observed (Gao et al., 2016). The first new peak (6) had a mass of 417.1789 $[M + H]^+$ with a predicted molecular formula of $C_{22}H_{26}NO_7$ (theoretical 417.1782 *m/z*), the second new peak (**7**) had a mass of 389.1368 $[M + H]^+$ with a predicted molecular formula of $C_{22}H_{18}N_3O_4$ (theoretical 389.1370 *m/z*), and the third new peak (**8**) had a mass of 390.1214 $[M + H]^+$ with a predicted molecular formula of $C_{22}H_{17}N_2O_5$ (theoretical 389.1210 *m/z*). We were unable to generate a sufficient quantity of these materials for further structural elucidation, despite multiple attempts. It is interestingly to note that nitrogenous phenalenones have been identified in the marine fungus *Coniothyrium cereale* albeit with different molecular formulas (Elsebai et al., 2016).

3.5. Perithecial pigment biosynthesis in F. Vanettenii

Based on our data and biosynthetic studies in other fungi, we propose that the perithecial pigment biosynthetic pathway (Fig. 8) starts similarly to the pathways for duclauxin and herqueinone (Gao et al., 2016; Gao et al., 2018). Biosynthesis for all three materials begins with the production of prephenalenone (**1**), which in *F. vanettenii* can spontaneously form dehydroxyprephenalenone (**2**). The next enzymatic step is the formation of phenalenone catalyzed by a monooxygenase, which can spontaneously form oxyphenalenone (**3**). In *Talaromyces stipitatus*, phenalenone undergoes four reductions catalyzed by DuxM, DuxJ, DuxD and DuxG to yield SF226 (Gao et al., 2018). We identified putative orthologs of DuxM, DuxJ and DuxD encoded by genes adjacent to *fsnI* in *F. vanettenii* that could modify phenalenone in a similar manner. The lack of a DuxG ortholog could be compensated for by an unrelated reductase, FsnP, encoded by a gene located adjacent to the *duxM* homolog *fsnM*. In *T. stipitatus*, SF226 forms a dimer which is further modified creating the final product duclauxin (Gao et al., 2018). In our study, we identified two compounds, corymbiferan lactone E and F, which are single (E) and double (F) O-methylation products of SF226, which we propose as possible final products of the biosynthetic pathway in *F. vanettenii*. We also propose that both O-methylations, at the C-7 and C-9 oxygens, are due to the activity of FsnK, a putative O-methyltransferase. The three remaining cluster genes not assigned to a biochemical step in this model where *fsnB*, encodes a putative oxidoreductase, and *fsnF* and *fsnQ*, encode proteins of unknown function. *fsnB* is the only gene of these three to share homology with a *T. stipitatus dux* gene, *duxB* (Gao et al., 2018). A role in duclauxin synthesis for DuxB is unclear although a homolog in *T. stipitatus*, *duxB'*, sharing 85 % sequence identity to *duxB* and located within a closely related *dux'* cluster, did convert 2 % of a penultimate intermediate into duclauxin (Gao et al., 2018). The putative oxidoreductase encoded by *fnsB* or the proteins of unknown function encoded by *fsnF* and *fsnQ* may play a non-essential role in corymbiferan lactone synthesis or perhaps contribute to creating the final red perithecial color.

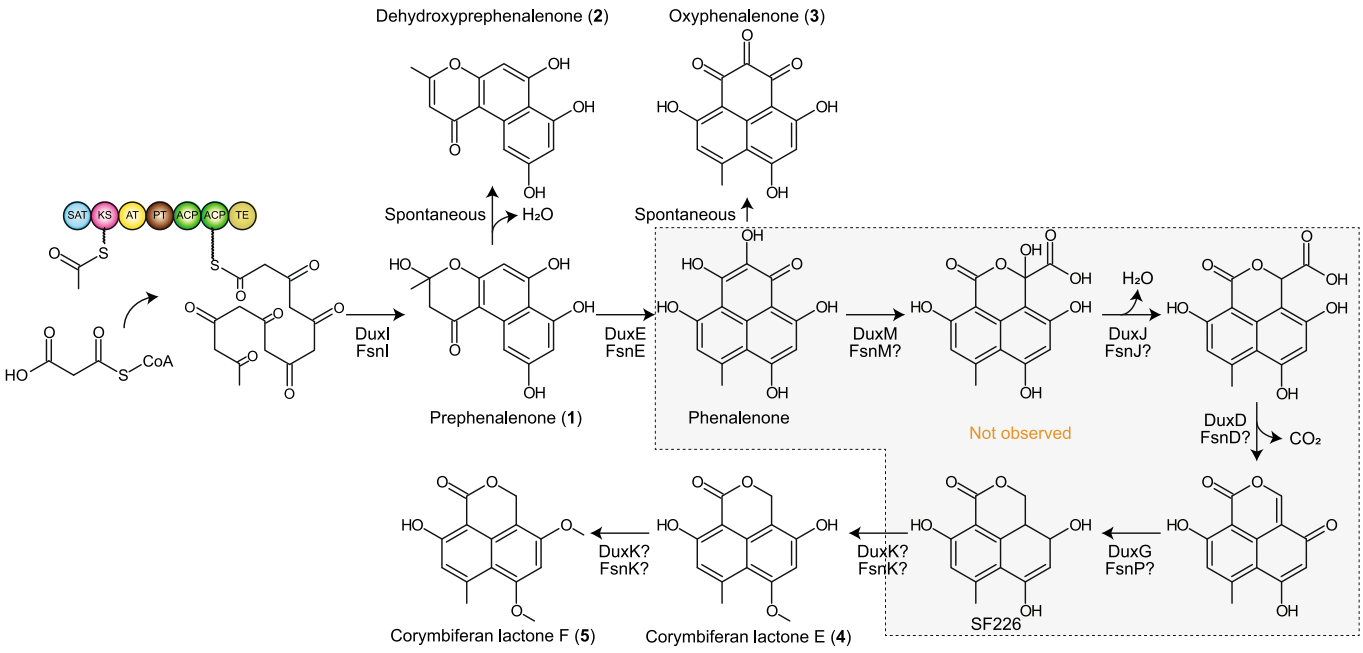

Fig. 8. Proposed biosynthesis of perithecial pigments in F. vanettenii based on our study and published pathways for duclauxin and herqueinone (Gao et al., 2016; Gao et al., 2018).

CRediT authorship contribution statement

Mikkel Rank Nielsen: Writing – review & editing, Writing – original draft, Methodology, Investigation, Conceptualization. **Trine Sørensen:** Writing – review & editing, Methodology, Investigation. **Tobias Bruun Pedersen:** Writing – review & editing, Investigation, Conceptualization. **Klaus Ringsborg Westphal:** Writing – review & editing, Writing – original draft, Investigation. **Lorena Díaz Fernández De Quincoces:** Writing – review & editing, Investigation. **Teis Esben Sondergaard:** Writing – review & editing, Investigation. **Reinhard Wimmer:** Writing – review & editing, Writing – original draft, Investigation. **Daren W. Brown:** Writing – review & editing, Writing – original draft, Methodology, Investigation. **Jens Laurids Sørensen:** Writing – review & editing, Writing – original draft, Supervision, Project administration, Funding acquisition, Conceptualization.

Declaration of competing interest

The authors declare that they have no known competing financial interests or personal relationships that could have appeared to influence the work reported in this paper.

Acknowledgements

The research was supported by grants from the Novo Nordisk Foundation (NNF15OC0016186 and NNF18OC0034952) and the Obel Family Foundation, Denmark. This research was also supported by the U.S. Department of Agriculture, Agricultural Research Service. Mention of trade names or commercial products in this publication is solely for the purpose of providing specific information and does not imply recommendation or endorsement by the U.S. Department of Agriculture. USDA is an equal opportunity provider and employer.

Appendix A. Supplementary data

Supplementary data to this article can be found online at https://doi.org/10.1016/j.fgb.2024.103912.

References

Arnstein, H. R. V., Cook, A. H., 1947. Production of antibiotics by fungi. Part III. Javanicin. An antibacterial pigment from *Fusarium javanicum*. J. Chem. Soc., 1021-1028.

Awakawa, T., Kaji, T., Wakimoto, T., Abe, I., 2012. A heptaketide naphthaldehyde produced by a polyketide synthase from *Nectria haematococca*. Bioorg. Med. Chem. Lett. 22, 4338–4340.

Bejenari, M., Nielsen, L., Spedtsberg, E.M.L., Nielsen, M.R., Pedersen, T.B., Sørensen, J.L., 2023. Yeast recombinational cloning for heterologous biosynthesis of polyketides: a molecular microbiology laboratory module for undergraduate students. Journal of Microbiology & Biology Education. 24, e00242–e322.

Brown, D.W., Kim, H.-S., McGovern, A.E., Probyn, C.E., Proctor, R.H., 2022. Genus-wide analysis of Fusarium polyketide synthases reveals broad chemical potential. Fungal Genetics and Biology. 160, 103696.

Brown, D.W., Proctor, R.H., 2016. Insights into natural products biosynthesis from analysis of 490 polyketide synthases from Fusarium. Fungal Genetics and Biology. 89, 37–51.

Bueno, C.J., Fischer, I.H., Rosa, D.D., Firmino, A.C., Harakava, R., Oliveira, C.M.G., Furtado, E.L., 2014. *Fusarium solani* f. sp *passiflorae*: a new forma specialis causing collar rot in yellow passion fruit. Plant Pathol. 63, 382–389.

Chung, W.C., Chen, L.W., Huang, J.H., Huang, H.C., Chung, W.H., 2011. A new 'forma specialis' of *Fusarium solani* causing leaf yellowing of Phalaenopsis. Plant Pathol. 60, 244–252.

Coleman, J.J., 2016. The *Fusarium solani* species complex: ubiquitous pathogens of agricultural importance. Mol. Plant Pathol. 17, 146–158.

Coleman, J.J., Rounsley, S.D., Rodriguez-Carres, M., Kuo, A., Wasmann, C.C., Grimwood, J., Schmutz, J., Taga, M., White, G.J., Zhou, S.G., Schwartz, D.C., Freitag, M., Ma, L.J., Danchin, E.G.J., Henrissat, B., Coutinho, P.M., Nelson, D.R., Straney, D., Napoli, C.A., Barker, B.M., Gribskov, M., Rep, M., Kroken, S., Molnar, I., Rensing, C., Kennell, J.C., Zamora, J., Farman, M.L., Selker, E.U., Salamov, A., Shapiro, H., Pangilinan, J., Lindquist, E., Lamers, C., Grigoriev, I.V., Geiser, D.M., Covert, S.F., Temporini, E., VanEtten, H.D., 2009. The genome of *Nectria haematococca*: Contribution of supernumerary chromosomes to gene expansion. PLoS Genet. 5.

Elsebai, M.F., Ghabbour, H.A., Mehiri, M., 2016. Unusual Nitrogenous Phenalenone Derivatives from the Marine-Derived Fungus Coniothyrium cereale. Molecules. 21, 178.

Frandsen, R.J.N., Nielsen, N.J., Maolanon, N., Sorensen, J.C., Olsson, S., Nielsen, J., Giese, H., 2006. The biosynthetic pathway for aurofusarin in *Fusarium graminearum* reveals a close link between the naphthoquinones and naphthopyrones. Molecular Microbiology. 61, 1069–1080.

Frandsen, R.J.N., Andersson, J.A., Kristensen, M.B., Giese, H., 2008. Efficient four fragment cloning for the construction of vectors for targeted gene replacement in filamentous fungi. BMC Mol, Biol, p. 9.

Frandsen, R.J.N., Rasmussen, S.A., Knudsen, P.B., Uhlig, S., Petersen, D., Lysøe, E., Gotfredsen, C.H., Giese, H., Larsen, T.O., 2016. Black perithecial pigmentation in *Fusarium* species is due to the accumulation of 5-deoxybostrycoidin-based melanin. Scientific Reports. 6, 26206.

Frisvad, J.C., 2012. Media and growth conditions for induction of secondary metabolite production. Methods in Molecular Biology (clifton N.J.). 944, 47–58.
Gao, S.S., Duan, A., Xu, W., Yu, P., Hang, L., Houk, K.N., Tang, Y., 2016. Phenalenone polyketide cyclization catalyzed by fungal polyketide synthase and flavin-dependent monooxygenase. Journal of the American Chemical Society. 138, 4249–4259.
Gao, S.S., Zhang, T., Garcia-Borràs, M., Hung, Y.S., Billingsley, J.M., Houk, K.N., Hu, Y., Tang, Y., 2018. Biosynthesis of Heptacyclic Duclauxins Requires Extensive Redox Modifications of the Phenalenone Aromatic Polyketide. J. Am. Chem. Soc. 140, 6991–6997.
Gómez-Cortecero, A., Harrison, R.J., Armitage, A.D., 2015. Draft genome sequence of a european isolate of the apple canker pathogen *Neonectria ditissima*. Genome Announcements. 3, e01243–e10315.
Graziani, S., Vasnier, C., Daboussi, M.J., 2004. Novel polyketide synthase from *Nectria haematococca*. Applied and Environmental Microbiology. 70, 2984–2988.
Hansen, F.T., Sørensen, J.L., Giese, H., Sondergaard, T.E., Frandsen, R.J., 2012. Quick guide to polyketide synthase and nonribosomal synthetase genes in *Fusarium*. Int. J. Food Microbiol. 155, 128–136.
Hansen, F.T., Gardiner, D.M., Lysøe, E., Fuertes, P.R., Tudzynski, B., Wiemann, P., Sondergaard, T.E., Giese, H., Brodersen, D.E., Sørensen, J.L., 2015. An update to polyketide synthase and non-ribosomal synthetase genes and nomenclature in *Fusarium*. Fungal Genetics and Biology. 75, 20–29.
Hardegger, E., Pfiffner, A., Steiner, K., Widmer, E., 1964. Welkstoffe und Antibiotika. Synthese von Javanicin-5,8-dimethyläther und Konstitution von Javanicin und Fusarubin. Helvetica Chimica Acta. 47, 2027–2200.
Harvey, C.J.B., Tang, M., Schlecht, U., Horecka, J., Fischer, C.R., Lin, H.-C., Li, J., Naughton, B., Cherry, J., Miranda, M., Li, Y.F., Chu, A.M., Hennessy, J.R., Vandova, G.A., Inglis, D., Aiyar, R.S., Steinmetz, L.M., Davis, R.W., Medema, M.H., Sattely, E., Khosla, C., St. Onge, R. P., Tang, Y., Hillenmeyer, M. E, 2018. HEx: A heterologous expression platform for the discovery of fungal natural products. Science Advances. 4.
Ibarra-Laclette, E., Sánchez-Rangel, D., Hernández-Domínguez, E., Pérez-Torres, C.A., Ortiz-Castro, R., Villafán, E., Alonso-Sánchez, A., Rodríguez-Haas, B., López-Buenfil, A., García-Avila, C., Ramírez-Pool, J.A., 2017. Draft Genome Sequence of the Phytopathogenic Fungus Fusarium euwallaceae, the Causal Agent of Fusarium Dieback. Genome Announc. 5.
Jørgensen, S.H., Frandsen, R.J.N., Nielsen, K.F., Lysøe, E., Sondergaard, T.E., Wimmer, R., Giese, H., Sørensen, J.L., 2014. *Fusarium graminearum PKS14* is involved in orsellinic acid and orcinol synthesis. Fungal Genetics and Biology. 70, 24–31.
Kakule, T.B., Sardar, D., Lin, Z.J., Schmidt, E.W., 2013. Two related pyrrolidinedione synthetase loci in *Fusarium heterosporum* ATCC 74349 produce divergent metabolites. ACS Chemical Biology. 8, 1549–1557.
Kim, W., Cavinder, B., Proctor, R.H., O'Donnell, K., Townsend, J.P., Trail, F., 2019. Comparative Genomics and Transcriptomics During Sexual Development Gives Insight Into the Life History of the Cosmopolitan Fungus Fusarium neocosmosporiellum. Front Microbiol. 10, 1247.
Kim, J.E., Han, K.H., Jin, H.M., Kim, H., Kim, J.C., Yun, S.H., Lee, Y.W., 2005. Putative polyketide synthase and laccase genes for biosynthesis of aurofusarin in Gibberella zeae. Applied and Environmental Microbiology. 71, 1701–1708.
Kolattukudy, P.E., Gamble, D.L., 1995. *Nectria haematococca*: pathogenesis and host specificity in plant diseases. In: Kohmoto, K. (Ed.), Pathogenesis and Host Specificity in Plant Pathogenic Fungi and Nematodes. Pergamon, Oxford, pp. 83–102.
Li, H., 2018. Minimap2: pairwise alignment for nucleotide sequences. Bioinformatics. 34, 3094–3100.
Linnemannstöns, P., Schulte, J., Prado, M.D., Proctor, R.H., Avalos, J., Tudzynski, B., 2002. The polyketide synthase gene pks4 from *Gibberella fujikuroi* encodes a key enzyme in the biosynthesis of the red pigment bikaverin. Fungal Genetics and Biology. 37, 134–148.
Malz, S., Grell, M.N., Thrane, C., Maier, F.J., Rosager, P., Felk, A., Albertsen, K.S., Salomon, S., Bohn, L., Schafer, W., Giese, H., 2005. Identification of a gene cluster responsible for the biosynthesis of aurofusarin in the *Fusarium graminearum* species complex. Fungal Genetics and Biology. 42, 420–433.
Mesny, F., Miyauchi, S., Thiergart, T., Pickel, B., Atanasova, L., Karlsson, M., Hüttel, B., Barry, K.W., Haridas, S., Chen, C., Bauer, D., Andreopoulos, W., Pangilinan, J., LaButti, K., Riley, R., Lipzen, A., Clum, A., Drula, E., Henrissat, B., Kohler, A., Grigoriev, I.V., Martin, F.M., Hacquard, S., 2021. Genetic determinants of endophytism in the Arabidopsis root mycobiome. Nature Communications. 12, 7227.
Nalim, F.A., Samuels, G.J., Wijesundera, R.L., Geiser, D.M., 2011. New species from the Fusarium solani species complex derived from perithecia and soil in the Old World tropics. Mycologia. 103, 1302–1330.
Nielsen, M.R., Holzwarth, A.K.R., Brew, E., Chrapkova, N., Kaniki, S.E.K., Kastaniegaard, K., Sorensen, T., Westphal, K.R., Wimmer, R., Sondergaard, T.E., Sorensen, J.L., 2019a. A new vector system for targeted integration and overexpression of genes in the crop pathogen *Fusarium solani*. Fungal Biol Biotechnol. 6, 25.
Nielsen, M.R., Kaniki, S.E.K., Sørensen, J.L., 2022. Targeted Genetic Engineering via *Agrobacterium*-Mediated Transformation in *Fusarium solani*. In: Skellam, E. (Ed.), Engineering Natural Product Biosynthesis: Methods and Protocols. Springer, US, New York, NY, pp. 93–114.
Nielsen, M.R., Sørensen, J.L., 2022. Investigating Fungal Biosynthetic Pathways Using Heterologous Gene Expression: Fusarium sp. as a Heterologous Host. In: Skellam, E. (Ed.), Engineering Natural Product Biosynthesis: Methods and Protocols. Springer, US, New York, NY, pp. 53–74.
Nielsen, M.R., Wollenberg, R.D., Westphal, K., Sondergaard, T.E., Wimmer, R., Gardiner, D.M., Sørensen, J.L., 2019b. Heterologous expression of intact biosynthetic gene clusters in Fusarium graminearum. Fungal Genetics and Biology. 132, 103248.
O'Donnell, K., 2000. Molecular phylogeny of the *Nectria haematococca-Fusarium solani* species complex. Mycologia. 92, 919–938.
O'Donnell, K., Sutton, D.A., Fothergill, A., McCarthy, D., Rinaldi, M.G., Brandt, M.E., Zhang, N., Geiser, D.M., 2008. Molecular phylogenetic diversity, multilocus haplotype nomenclature, and in vitro antifungal resistance within the *Fusarium solani* species complex. Journal of Clinical Microbiology. 46, 2477–2490.
Parisot, D., Devys, M., Barbier, M., 1990. Naphthoquinone pigments related to fusarubin from the fungus *Fusarium solani* (Mart.) Sacc. Microbios. 64, 31–47.
Pedersen, T.B., Nielsen, M.R., Kristensen, S.B., Spedtsberg, E.M.L., Yasmine, W., Matthiesen, R., Sørensen, T., Petersen, C., Muff, J., Sondergaard, T.E., Nielsen, K.L., Wimmer, R., Sørensen, J.L., 2020. Heterologous Expression of the Core Genes in the Complex Fusarubin Gene Cluster of *Fusarium Solani*. International Journal of Molecular Sciences. 21, 7601.
Pedersen, T.B., Nielsen, M.R., Kristensen, S.B., Spedtsberg, E.M.L., Sørensen, T., Petersen, C., Muff, J., Sondergaard, T.E., Nielsen, K.L., Wimmer, R., Gardiner, D.M., Sørensen, J.L., 2022. Speed Dating for Enzymes! Finding the Perfect Phosphopantetheinyl Transferase Partner for Your Polyketide Synthase. Mirobial Cell Factories. 21, 9.
Petersen, C., Sørensen, T., Westphal, K.R., Fechete, L.I., Sondergaard, T.E., Sørensen, J.L., Nielsen, K.L., 2022. High molecular weight DNA extraction methods lead to high quality filamentous ascomycete fungal genome assemblies using Oxford Nanopore sequencing. Microb Genom. 8.
Petersen, C., Sørensen, T., Nielsen, M.R., Sondergaard, T.E., Sørensen, J.L., Fitzpatrick, D. A., Frisvad, J.C., Nielsen, K.L., 2023. Comparative genomic study of the Penicillium genus elucidates a diverse pangenome and 15 lateral gene transfer events. IMA Fungus. 14, 3.
Pokhrel, A., Coleman, J.J., 2023. Inventory of the Secondary Metabolite Biosynthetic Potential of Members within the Terminal Clade of the Fusarium solani Species Complex. Journal of Fungi. 9, 799.
Ren, J.W., Zhang, F., Liu, X.Y., Li, L., Liu, G., Liu, X.Z., Che, Y.S., 2012. Neonectrolide A, a new oxaphenalenone spiroketal from the fungus *Neonectria* sp. Org. Lett. 14, 6226–6229.
Ren, J.W., Niu, S.B., Li, L., Geng, Z.F., Liu, X.Z., Che, Y.S., 2015. Identification of oxaphenalenone ketals from the ascomycete fungus *Neonectria* sp. Journal of Natural Products. 78, 1316–1321.
Robien, W., 2017. A Critical Evaluation of the Quality of Published 13C NMR Data in Natural Product Chemistry. In: Kinghorn, A.D. (Ed.), Progress in the Chemistry of Organic Natural Products 105. Springer International Publishing, Cham, pp. 137–215.
Ruelius, H.W., Gauhe, A., 1950. Über Fusarubin, einen Naphthochinonfarbstoff aus Fusarien. Annalen Der Chemie-Justus Liebig. 569, 38–59.
Severinsen, M.M., Westphal, K.R., Terp, M., Sørensen, T., Olsen, A., Bachleitner, S., Studt-Reinhold, L., Wimmer, R., Sondergaard, T.E., Sørensen, J.L., 2023. Filling out the gaps – identification of fugralins as products of the PKS2 cluster in Fusarium graminearum. Frontiers in Fungal Biology. 4.
Šišić, A., Al-Hatmi, A.M.S., Baćanović-Šišić, J., Ahmed, S.A., Dennenmoser, D., de Hoog, G.S., Finckh, M.R., 2018a. Two new species of the *Fusarium solani* species complex isolated from compost and hibiscus (*Hibiscus* sp.). Antonie Van Leeuwenhoek. 111, 1785–1805.
Šišić, A., Baćanović-Šišić, J., Al-Hatmi, A.M.S., Karlovsky, P., Ahmed, S.A., Maier, W., de Hoog, G.S., Finckh, M.R., 2018b. The 'forma specialis' issue in *Fusarium*: A case study in *Fusarium solani* f. sp. *pisi*. Scientific Reports. 8, 1252.
Smedsgaard, J., 1997. Micro-scale extraction procedure for standardized screening of fungal metabolite production in cultures. Journal of Chromatography a. 760, 264–270.
Sørensen, J.L., Sondergaard, T.E., 2014. The effects of different yeast extracts on secondary metabolite production in Fusarium. Int. J. Food Microbiol. 170, 55–60.
Studt, L., Wiemann, P., Kleigrewe, K., Humpf, H.-U., Tudzynski, B., 2012. Biosynthesis of fusarubins accounts for pigmentation of *Fusarium fujikuroi* perithecia. Applied and Environmental Microbiology. 78, 4468–4480.
Suga, H., Ikeda, S., Taga, M., Kageyama, K., Hyakumachi, M., 2002. Electrophoretic karyotyping and gene mapping of seven formae speciales in *Fusarium solani*. Curr. Genet. 41, 254–260.
Sullivan, M.J., Petty, N.K., Beatson, S.A., 2011. Easyfig: a genome comparison visualizer. Bioinformatics. 27, 1009–1010.
Tamura, K., Stecher, G., Kumar, S., 2021. MEGA11: Molecular Evolutionary Genetics Analysis Version 11. Mol Biol Evol. 38, 3022–3027.
Twaruschek, K., Spörhase, P., Michlmayr, H., Wiesenberger, G., Adam, G., 2018. New plasmids for *Fusarium* transformation allowing positive-negative selection and efficient Cre-loxP mediated marker recycling. Front Microbiol. 9, 1954.
Von Bargen, K.W., Niehaus, E.M., Bergander, K., Brun, R., Tudzynski, B., Humpfir, H.U., 2013. Structure elucidation and antimalarial activity of apicidin F: An apicidin-like compound produced by *Fusarium fujikuroi*. Journal of Natural Products. 76, 2136–2140.
Westphal, K.R., Werner, M.I.H., Nielsen, K.A.H., Sørensen, J.L., Andrushchenko, V., Winde, J., Hertz, M., Jensen, M.A., Mortensen, M.L., Bouř, P., Sondergaard, T.E., Wimmer, R., 2019. Characterization of Eight Novel Spiroleptosphols from *Fusarium avenaceum*. Molecules. 24, 3498.
Wiemann, P., Willmann, A., Straeten, M., Kleigrewe, K., Beyer, M., Humpf, H.U., Tudzynski, B., 2009. Biosynthesis of the red pigment bikaverin in *Fusarium fujikuroi*: genes, their function and regulation. Molecular Microbiology. 72, 931–946.
Wollenberg, R.D., Saei, W., Westphal, K.R., Klitgaard, C.S., Nielsen, K.L., Lysøe, E., Gardiner, D.M., Wimmer, R., Sondergaard, T.E., Sørensen, J.L., 2017. Chrysogine

biosynthesis is mediated by a two-module nonribosomal peptide synthetase. Journal of Natural Products. 80, 2131–2135.
Xie, S.Y., Ma, T., Zhao, N., Zhang, X., Fang, B., Huang, L., 2022. Whole-Genome Sequencing and Comparative Genome Analysis of Fusarium solani-melongenae Causing Fusarium Root and Stem Rot in Sweetpotatoes. Microbiol Spectr. 10, e0068322.
Zhang, N., O'Donnell, K., Sutton, D.A., Nalim, F.A., Summerbell, R.C., Padhye, A.A., Geiser, D.M., 2006. Members of the *Fusarium solani* species complex that cause infections in both humans and plants are common in the environment. Journal of Clinical Microbiology. 44, 2186–2190.